

1 **Supplementary information for: SARS-CoV-2 mechanistic correlates of protection: insight**
2 **from modelling response to vaccines**

3

4

5 **Authors:** Marie Alexandre, Romain Marlin, Mélanie Prague, Séverin Coleon, Nidhal Kahlaoui,
6 Sylvain Cardinaud, Thibaut Naninck, Benoit Delache, Mathieu Surenaud, Mathilde Galhaut,
7 Nathalie Dereuddre-Bosquet, Mariangela Cavarelli, Pauline Maisonnasse, Mireille Centlivre,
8 Christine Lacabaratz, Aurelie Wiedemann, Sandra Zurawski, Gerard Zurawski, Olivier
9 Schwartz, Rogier W Sanders, Roger Le Grand, Yves Levy, Rodolphe Thiébaud

10

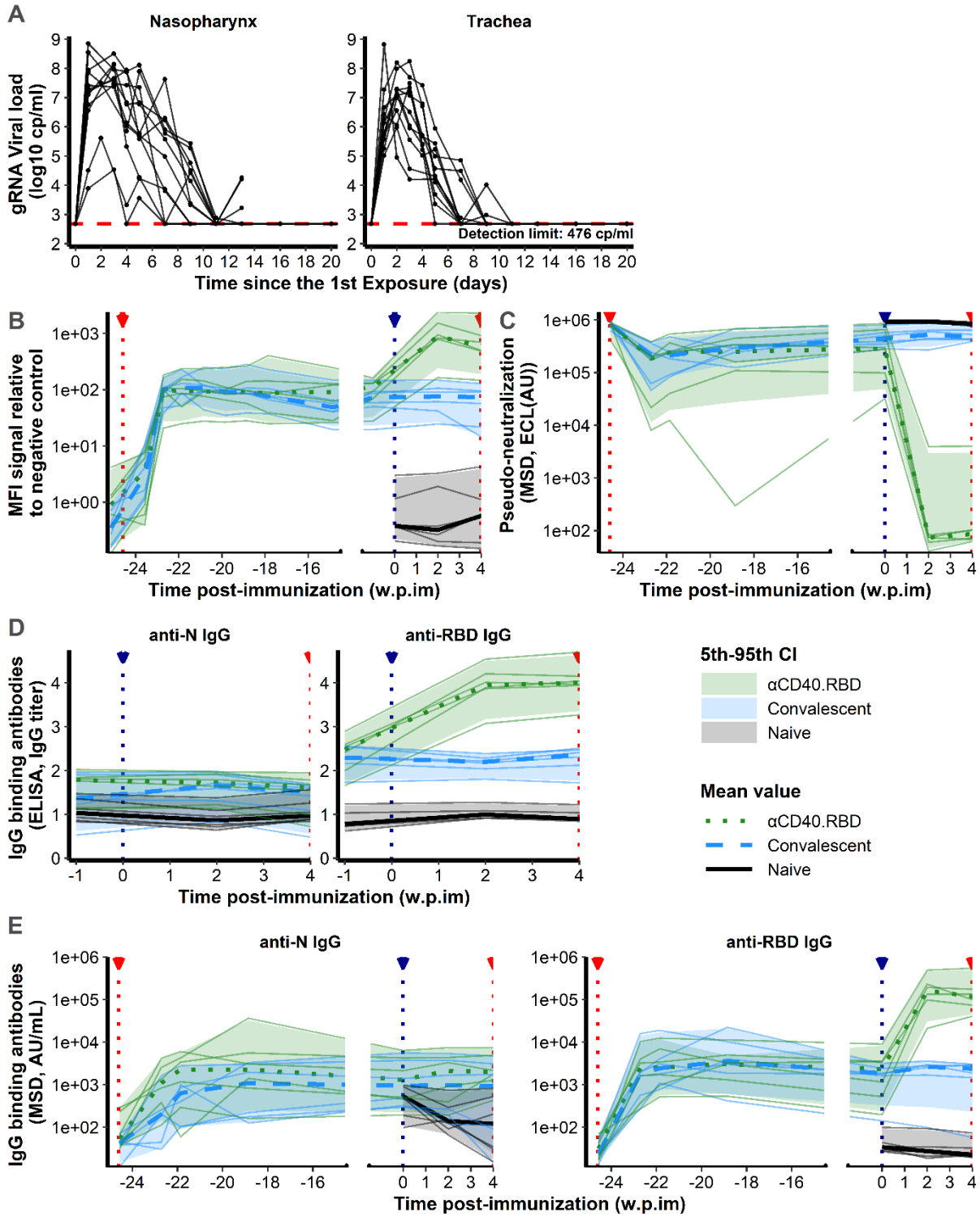
11 *Corresponding author: Prof Rodolphe Thiébaud

12 Bordeaux University, Departement of Public Health

13 146 Rue Leo Saignat, 33076 Bordeaux Cedex, France

14 rodolphe.thiebaut@u-bordeaux.fr

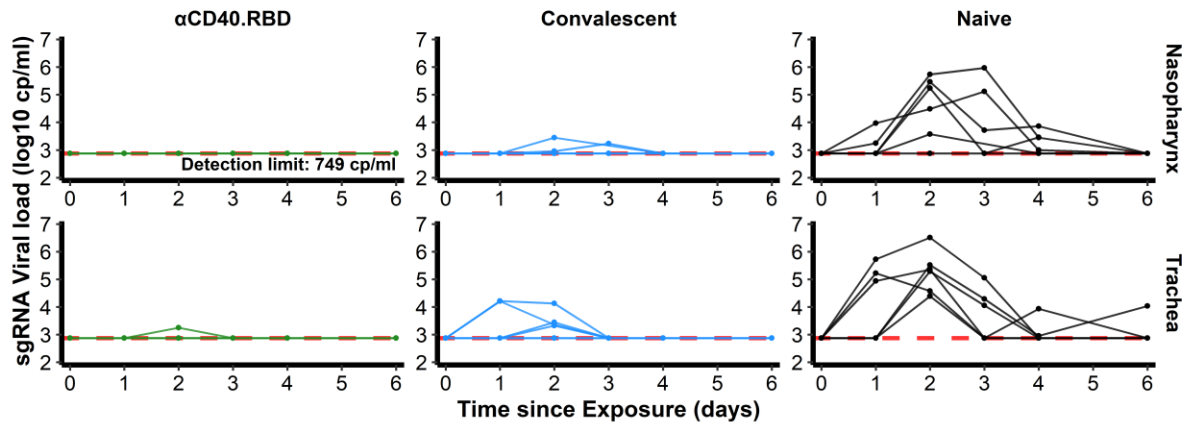
15 **Supplementary Figures and Tables**



17 **Fig. S1. Viral dynamics after the first exposure to SARS-CoV-2 and biomarker**
18 **measurements from the first to the second exposure to SARS-CoV-2.**

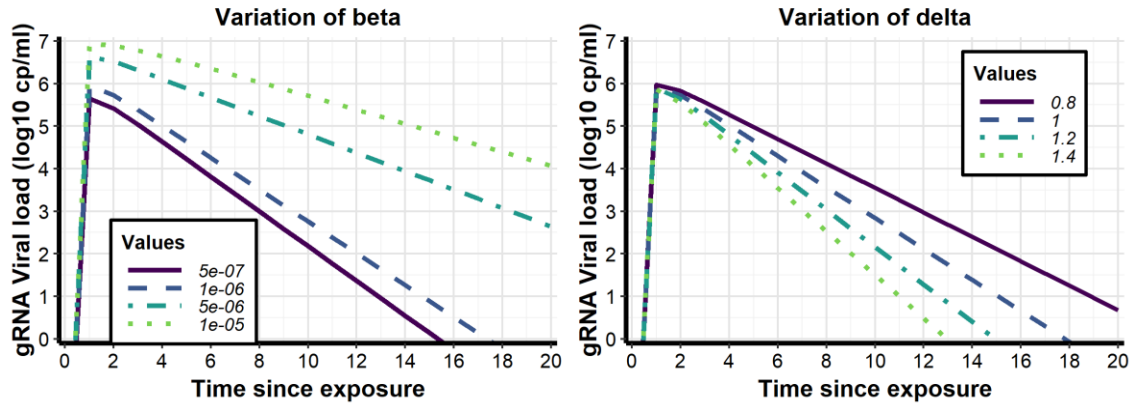
19 (A) Individual log₁₀ transformed gRNA viral load dynamics in nasopharyngeal (left) and
20 tracheal (right) swabs after the initial exposure to SARS-CoV-2 in naive macaques (n=12). Solid
21 lines represent individual values. Horizontal red dashed lines indicate the limit of quantification.
22 (B) Relative MFI of IgG binding to SARS-CoV-2 Spike protein, measured using a Luminex-
23 based serology assay, in serum samples, after the initial exposure to SARS-CoV-2. (C)
24 Quantification of antibodies inhibiting the attachment of Spike protein to ACE2 receptor in NHP
25 serum, measured by the Mesoscale Discovery (MSD, Rockville, MD) pseudo-neutralization
26 assay. Results are expressed as ECL (ECL, Electro-chemiluminescence) in AU. (D)
27 Quantification of SARS-CoV-2 IgG binding N or RBD domain measured in the serum of NHPs
28 titrated by ELISA assay. Results are expressed in IgG titer. (E) Quantification of SARS-CoV-2
29 IgG binding N and RBD domain measured in the serum of NHPs using a multiplexed solid-
30 phase chemiluminescence assay. Results are expressed in AU/mL. (B-E) Results are obtained
31 after the initial exposure to SARS-CoV-2 at -24.9 weeks post-immunization (w.p.im) in
32 convalescent (n=6, blue, dashed line) and α CD40.RBD-vaccinated convalescent (n=6, green,
33 dotted line) animals and at 4 w.p.im in naive (n=6, black, solid line) animals. Thin lines represent
34 individual values. Thick lines indicate medians within each group and shaded areas indicate 5th-
35 95th confidence intervals. The red (-24.6 and 4.0 w.p.im) and blue (0 w.p.im) lines highlight viral
36 exposure and vaccination respectively.

37



38
39

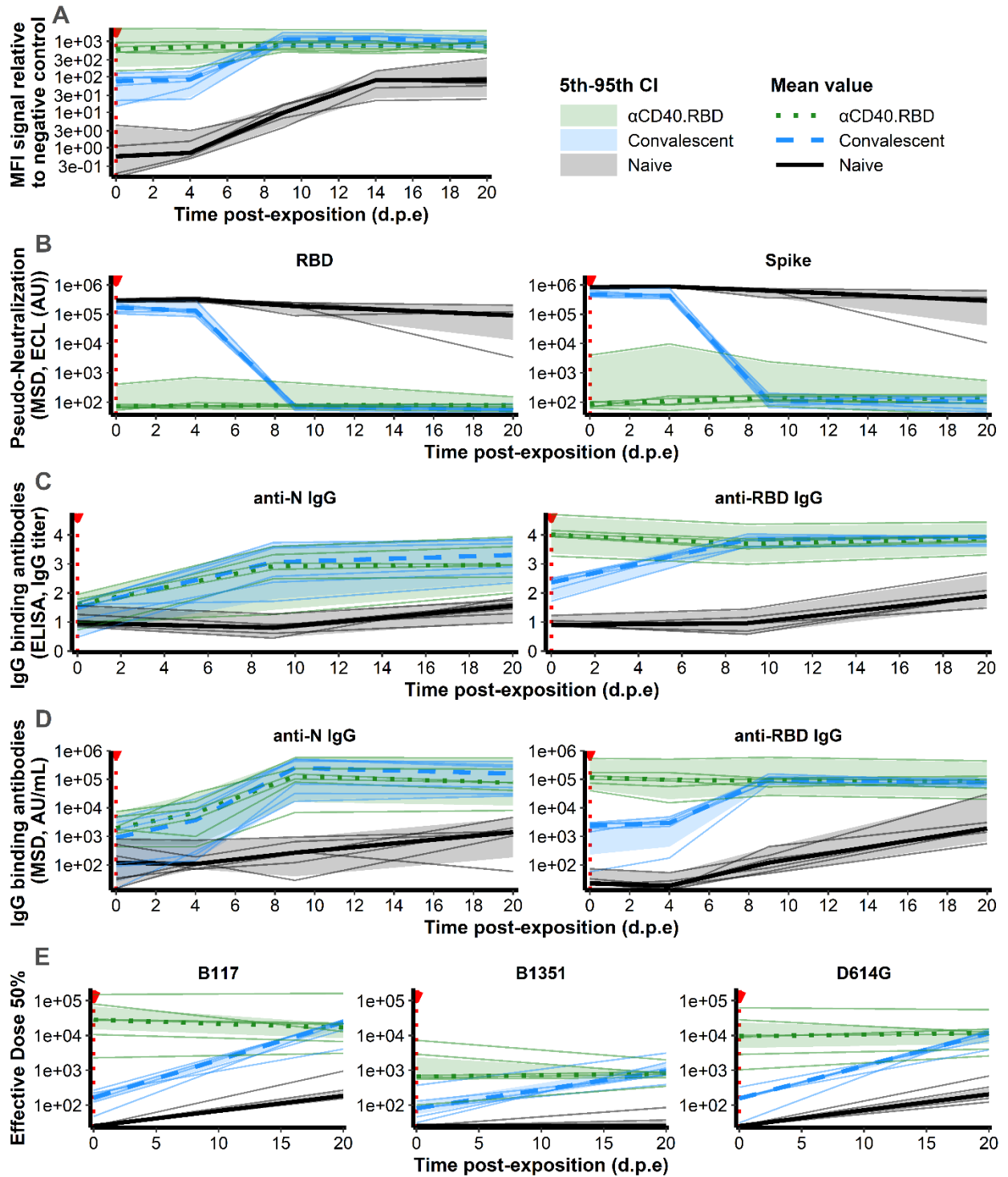
40 Individual log₁₀ transformed subgenomic (gRNA) viral load dynamics in nasopharyngeal (top)
 41 and tracheal (bottom) swabs after the initial exposure to SARS-CoV-2 in naive macaques (n=6,
 42 black, right) and after the second exposure in convalescent (n=6, blue, middle) and α CD40.RBD-
 43 vaccinated convalescent (n=6, green, left) groups. Horizontal red dashed lines indicate the limit
 44 of quantification.



45

46 **Fig. S3. Modelling of the viral dynamics using mechanistic model**

47 Examples simulated genomic viral load dynamics for different values of viral infectivity (β , left)
 48 or loss rate of infected cells (δ , right) showing the effect of either blocking de novo infection or
 49 promoting the destruction of infected cells on viral dynamics profile. Except for β or δ , all other
 50 parameters were fixed at a given value.



52 **Fig. S4. Antibody measurements after the second exposure to SARS-CoV-2**

53 (A) Relative MFI of IgG binding to SARS-CoV-2 Spike protein, measured using a Luminex-

54 based serology assay, in serum samples, after the second exposure to SARS-CoV-2. (B)

55 Quantification of antibodies inhibiting that attachment of RBD domain or Spike protein to ACE2

56 receptor in NHP serum, measured by the Mesoscale Discovery (MSD, Rockville, MD) pseudo-

57 neutralization assay, after the second exposure to SARS-CoV-2. Results are expressed as ECL,

58 in AU. (C) Quantification of SARS-CoV-2 IgG binding N or RBD domain measured in the

59 serum of NHPs titrated by ELISA assay, after the second exposure to SARS-CoV-2. Results are

60 expressed in Ig titer. (D) Quantification of SARS-CoV-2 IgG binding N or RBD domain

61 measured in the serum of NHPs using a multiplexed solid-phase chemiluminescence assay, after

62 the second exposure to SARS-CoV-2. Results are expressed in AU/mL. (E) Quantification of

63 neutralizing antibodies against B.1.1.7, B.1.351 and D614G SARS-CoV-2 strains measured in

64 the serum of NHPs using S-Fuse neutralization assay, after the second exposure to SARS-CoV-2

65 (measured only at the exposure and 20 days post-exposure (d.p.e)). Results are expressed as

66 ED50 (Effective dose 50%). (A-E) Results are obtained after the initial exposure to SARS-CoV-

67 2 in naive macaques (n=6, black, solid line) and after the second exposure in convalescent (n=6,

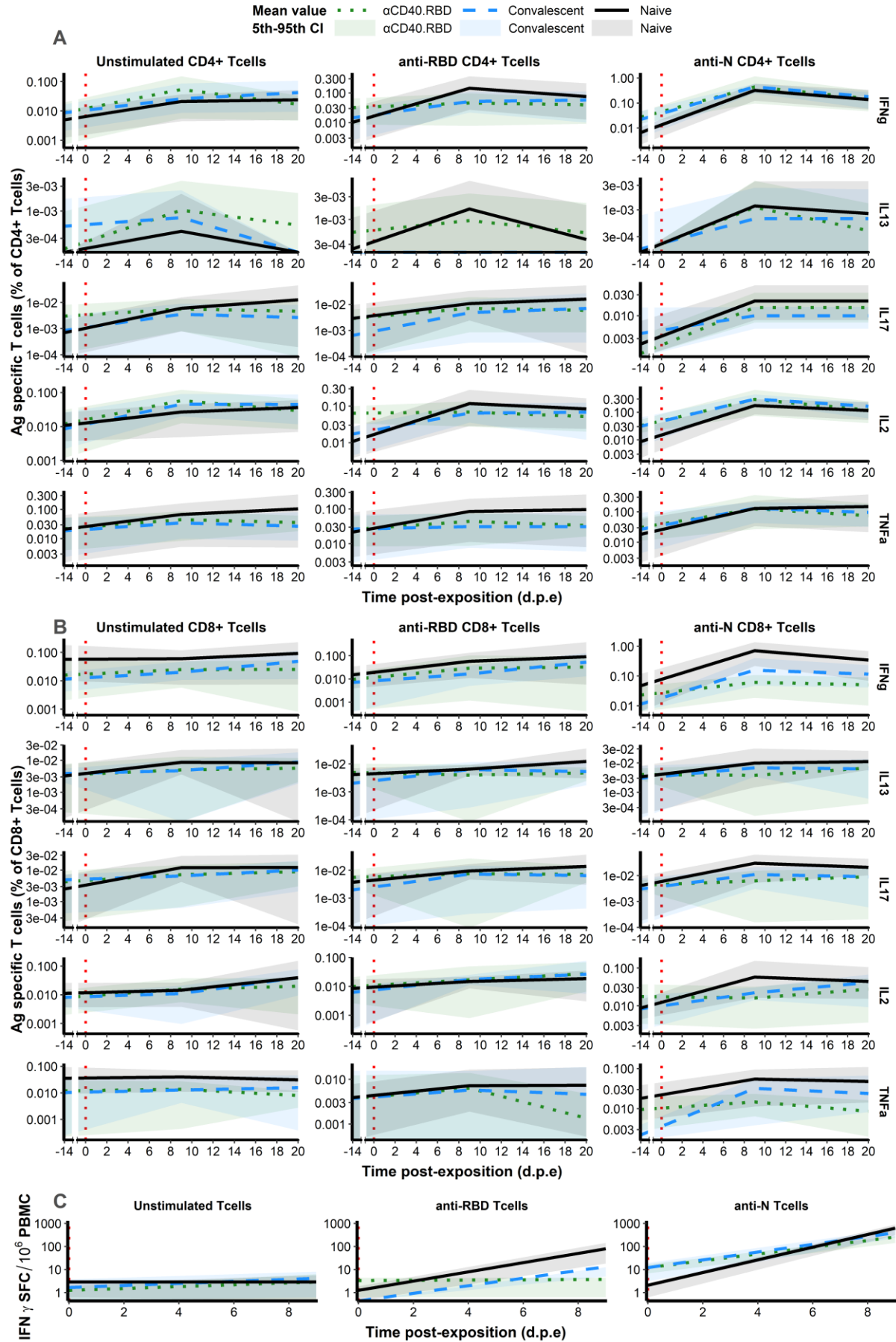
68 blue, dashed line) and α CD40.RBD-vaccinated convalescent (n=6, green, dotted line) animals.

69 Thin lines represent individual values. Thick lines indicate medians within each group and

70 shaded areas indicate 5th-95th confidence intervals. Red dotted vertical lines highlight the viral

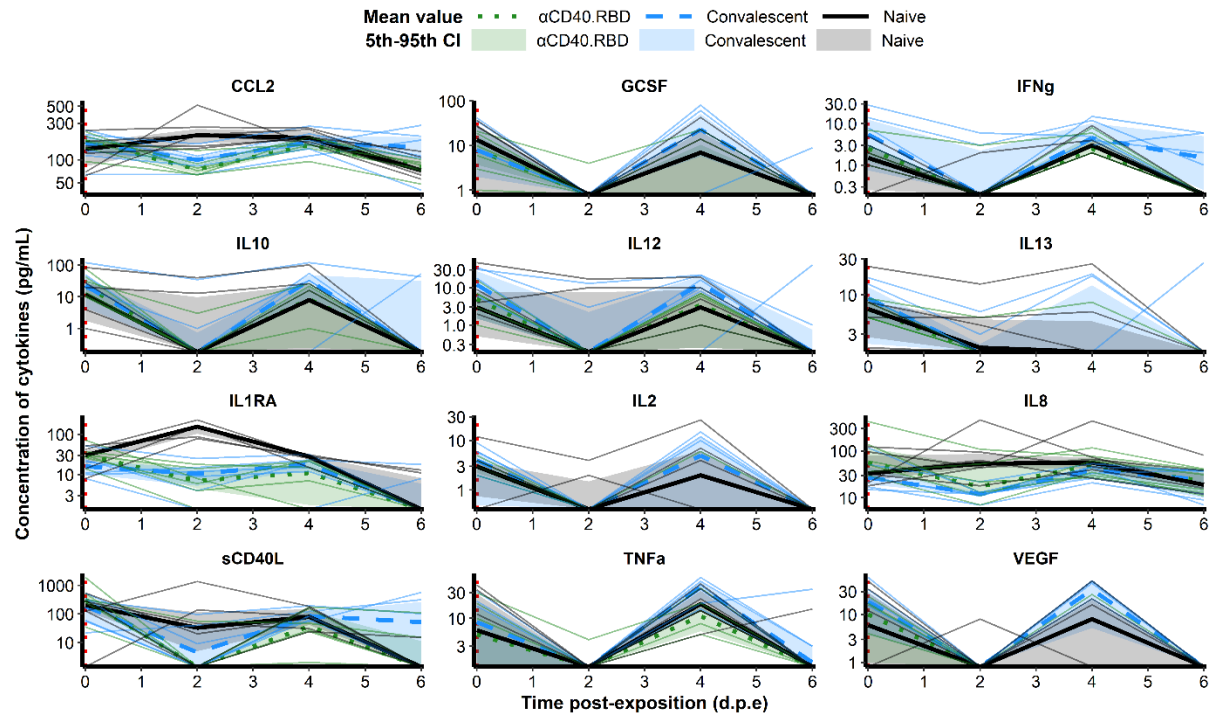
71 exposure.

72



74 **Fig. S5. Antigen-specific T-cell responses in NHPs after the second exposure to SARS-**
75 **CoV-2**

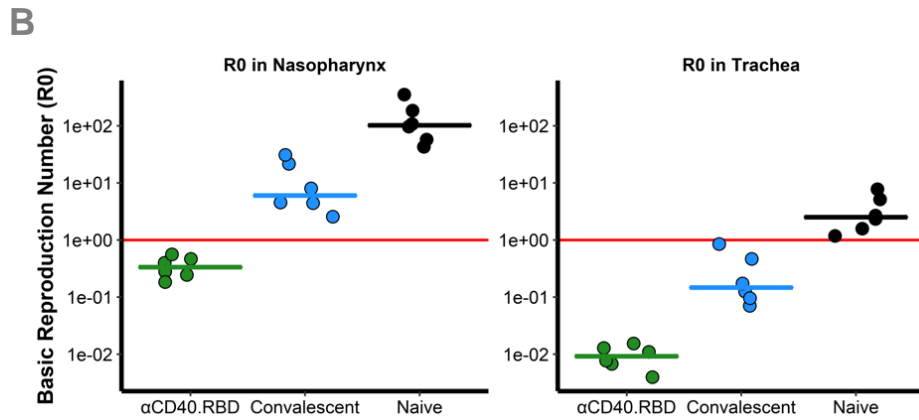
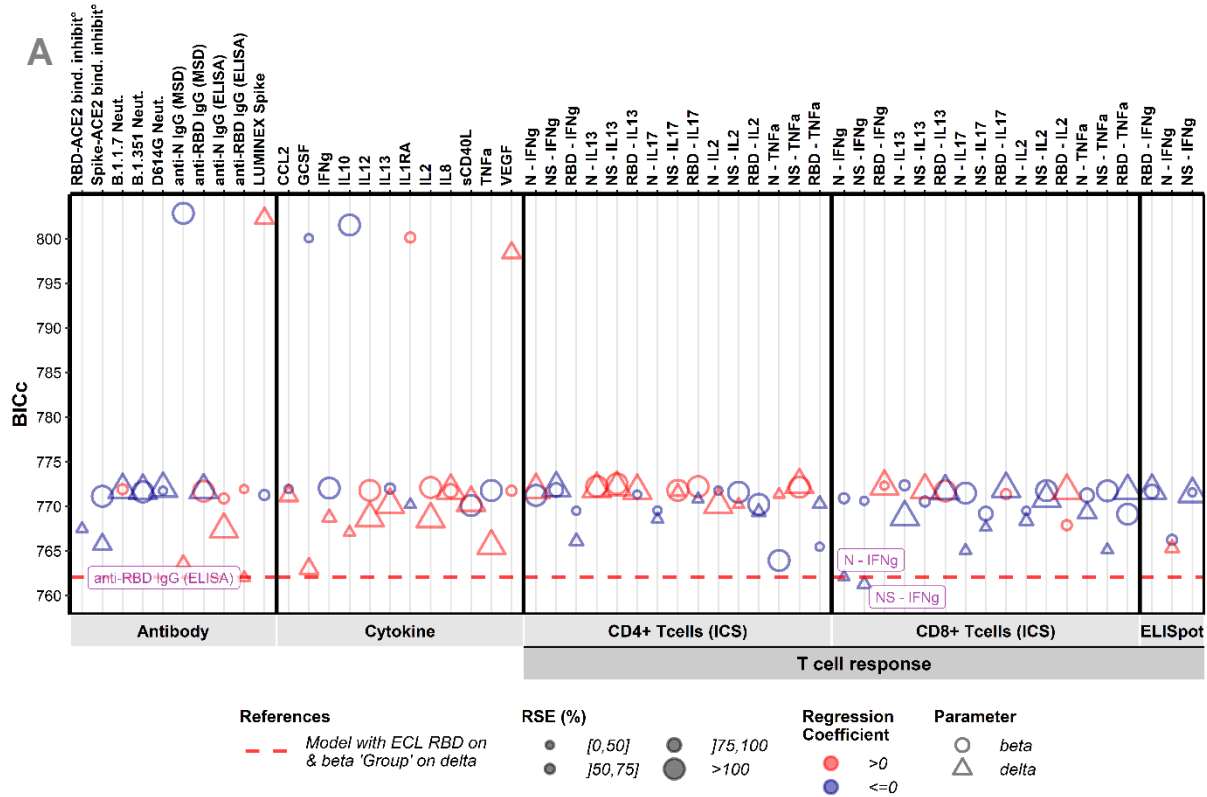
76 **(A-B)** Frequency of IFN γ ⁺ (first line), IL-13⁺ (second line), IL-17⁺ (third line), IL-2⁺ (fourth line)
77 or TNF α ⁺ (fifth line) antigen-specific CD4⁺ Tcells (CD154⁺) and CD8⁺ Tcells (CD137⁺) in the
78 total CD4⁺ Tcell (A) or CD8⁺ Tcell (B) population in NHP serum. PBMCs were stimulated *ex-*
79 *vivo* overnight with medium (left), SARS-CoV-2 RBD (middle) or N (right) overlapping peptide
80 pools. T-cell responses being not measured at the challenge, measured obtained 14 days pre-
81 exposure were added. **(C)** Antigen-specific T-cell responses in NHPs. T-cells were analyzed by
82 ELISpot after *ex-vivo* stimulation with SARS-CoV-2 RBD or N overlapping peptide pools and
83 plotted as spot-forming cells (SFC) per 1.0x10⁶ PBMCs. **(A-C)** Results are obtained after the
84 initial exposure to SARS-CoV-2 in naive macaques (n=6, black, solid line) and after the second
85 exposure in convalescent (n=6, blue, dashed line) and α CD40.RBD-vaccinated convalescent
86 (n=6, green, dotted line) animals. Thin lines represent individual values. Thick lines indicate
87 medians within each group and shaded areas indicate 5th-95th confidence intervals. Red dotted
88 vertical lines highlight the viral exposure.



89

90 **Fig. S6. Cytokines and chemokines in the plasma in NHPs after the second exposure to**
 91 **SARS-CoV-2**

92 Plasma concentration of 12 cytokines and chemokines in pg/mL. Results are obtained after the
 93 initial exposure to SARS-CoV-2 in naive macaques (n=6, black, solid line) and after the second
 94 exposure in convalescent (n=6, blue, dashed line) and α CD40.RBD-vaccinated convalescent
 95 (n=6, green, dotted line) animals. Thin lines represent individual values. Thick lines indicate
 96 medians within each group and shaded areas indicate 5th-95th confidence intervals. Red dotted
 97 vertical lines highlight the viral exposure.



98

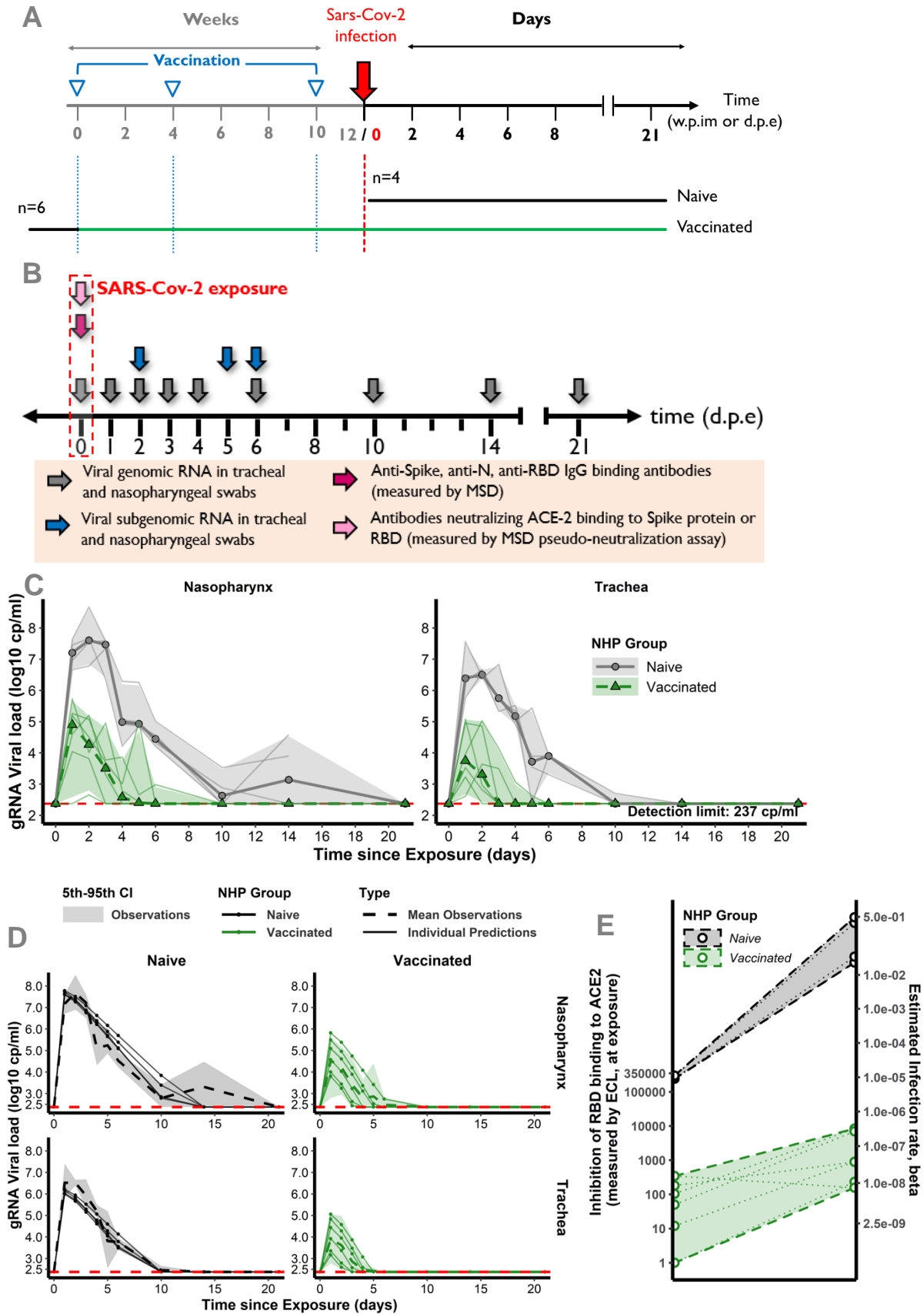
99

100 **Fig. S7. Immune markers selection and Basic reproduction number**

101 (A) Systematic screening of effect of the markers (Step 2). For every single marker, a model,
 102 already adjusted on viral infectivity with antibodies inhibiting the attachment of RBD domain to
 103 ACE2 receptor, has been fitted to explore whether it explains the variation of the parameter of
 104 interest better or as well than the model of reference. Parameters of interest were β , the infection

105 rate of ACE2+ target cells and δ , the loss rate of infected cells. Models were compared according
106 to the Bayesian Information Criterion (BIC), the lower being the better. The red dashed line
107 represents the reference model that includes the group effect (naive/ convalescent/vaccinated) on
108 the parameter δ and with adjustment of pseudo-neutralization on β . **(B)** *Reproduction rate at the*
109 *time of exposure*. Model predictions of the reproduction rate at the time of exposure (R_0) in the
110 tracheal (right) and nasopharyngeal (left) compartments for naive (black), convalescent (blue)
111 and α CD40.RBD-vaccinated convalescent (green) animals. The reproduction rate is representing
112 the number of infected cells from one infected cell if target cells are unlimited. When this
113 effective reproduction rate is below 1, it means that the infection is going to be cured. The
114 values of R_0 were estimated by the model with viral infectivity (β) and loss rate of infected cells
115 (δ) adjusted on pseudo-neutralization and anti-RBD IgG binding antibodies titrated by ELISA
116 assay respectively measured only at the time of challenge. Horizontal solid red lines highlight the
117 threshold of the reproduction rate equals to one.

118



120 **Fig. S8. The second study testing two-component spike nanoparticle vaccine.**

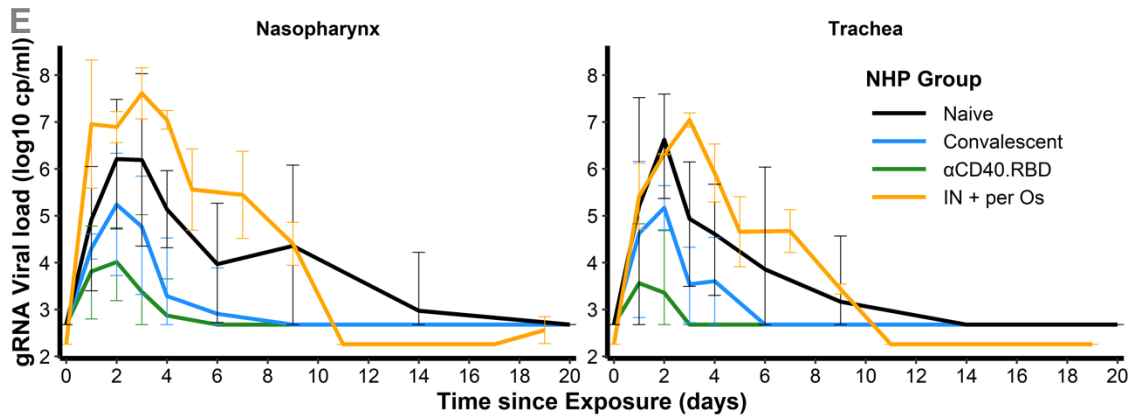
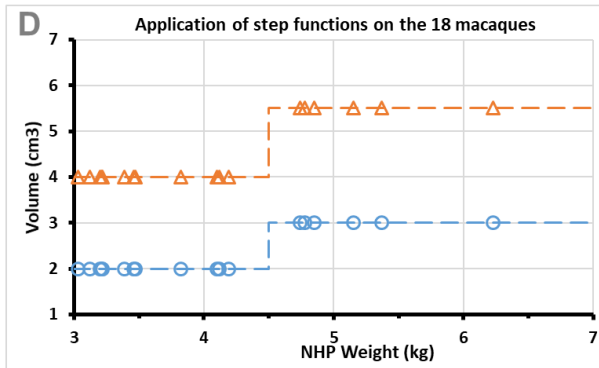
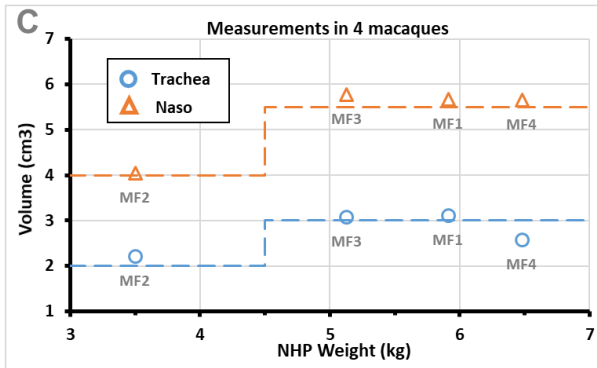
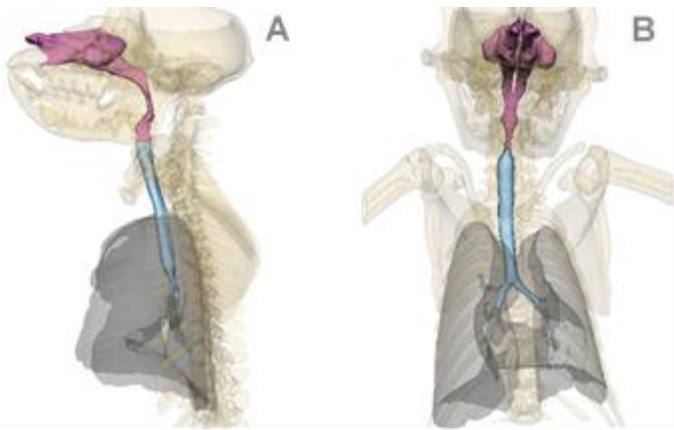
121 (A) *Study design.* Cynomolgus macaques were randomly assigned in two experimental groups.
122 Twelve, eight and two weeks post-infection with SARS-CoV-2 virus, six of them were
123 successively immunized with 50 µg of SARS-CoV-2 S-I53-50NP vaccine. The four other
124 animals received no vaccination. Two weeks after the final immunization, all monkeys were
125 exposed to a total dose of 10^6 pfu of SARS-CoV-2 virus via intra-nasal and intra-tracheal routes.
126 (B) *Harvest times and measurements.* Nasopharyngeal and tracheal fluids were collected at 0, 1,
127 2, 3, 4, 5, 6, 10, 14 and 21 d.p.e while blood was taken at 0, 2, 4, 6, 10, 14 and 21 d.p.e. Genomic
128 and subgenomic viral loads were measured by RT-qPCR. Anti-Spike, anti-RBD and anti-
129 Nucleocapside (N) IgG were titrated using a multiplexed immunoassay developed by Mesoscale
130 Discovery (MSD, Rockville, MD) and expressed in AU/mL. The MSD pseudo-neutralization
131 assay was used to quantify antibodies neutralizing the binding of the spike protein and RBD
132 domain to the ACE2 receptor and results were expressed in ECL. (C) Genomic viral load
133 dynamics in nasopharyngeal and tracheal swabs after the exposure to SARS-Cov-2 in naïve
134 (black, solid line) and vaccinated (green, dashed line) animals. Thin lines represent individual
135 values. Thick lines indicate medians within each group. (D) Model fit to the log₁₀-transformed
136 observed gRNA viral load in nasopharynx and trachea after the exposure to SARS-CoV-2 in
137 naïve and vaccinated macaques. Solid thin lines indicate individual dynamics predicted by the
138 model adjusted for groups. Thick dashed lines indicate mean viral load over time. (E) *Thresholds*
139 *of inhibition of RBD-ACE2 binding.* Estimated infection rate of target cells ($(\text{copies/mL})^{-1}\text{day}^{-1}$)
140 according to the quantification of antibodies inhibiting RBD-ACE2 binding (ECL) at exposure
141 for naïve (black) and vaccinated (green) animals. Thin dotted lines and circles represent
142 individual infection rates (right axis) and neutralizing antibodies (left axis). Thick dashed lines

143 and dashed areas delimit the pseudo-neutralization / viral infectivity relationships within each
144 group. (C,D) Horizontal red dashed lines represent the limit of quantification and shaded areas
145 the 95% confidence intervals.

146

147

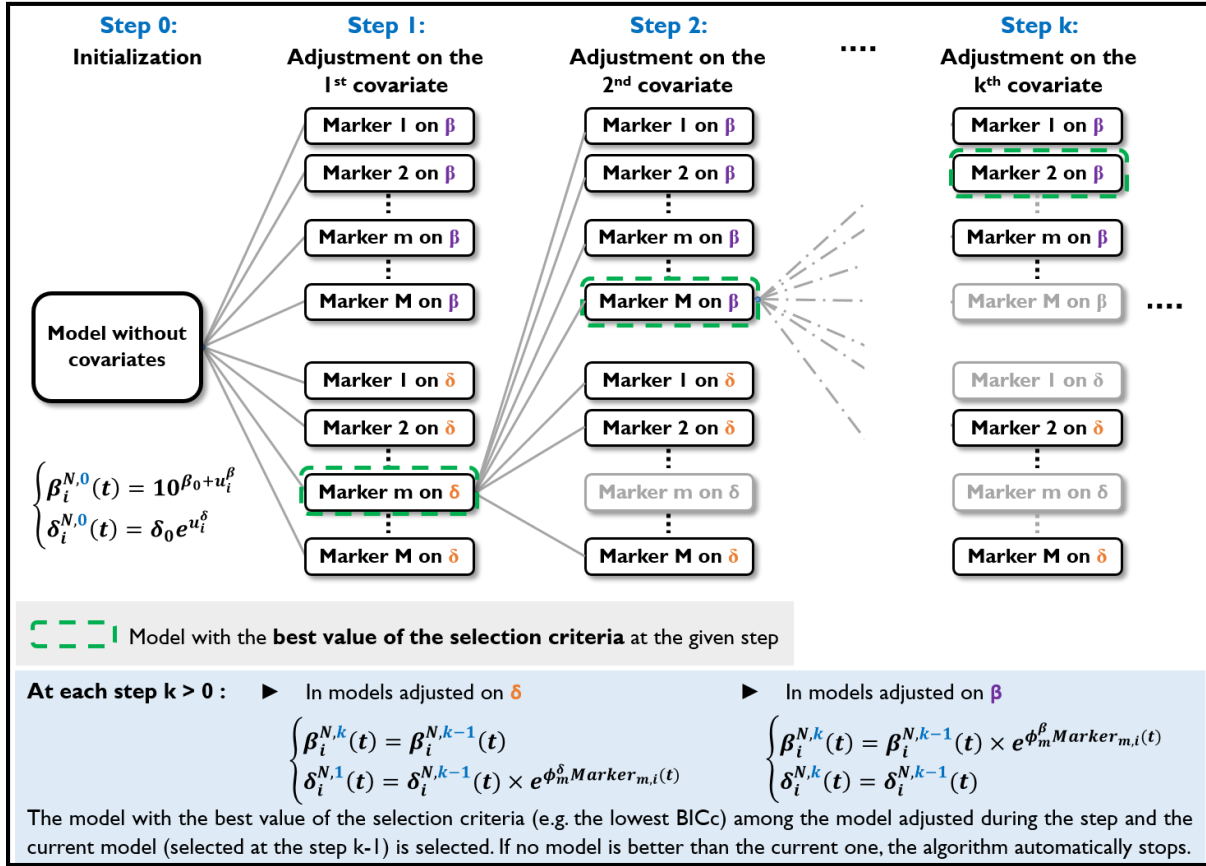
148



150 **Fig. S9. Modelling of the dynamics of viral replication**

151 **(A)** Sagittal view of the 3D representation of the NHP respiratory system. **(B)** Coronal view of
152 the 3D representation of the NHP respiratory system. (A-B) Lungs are colored in grey, Trachea
153 and Nasal regions in blue and purple respectively. **(C)** Relationship between the weights (in kgs)
154 measured in 4 NHPs and the estimation of the volume of their tracheal (blue circles) and nasal
155 (orange triangles) regions (in cm^3). Measurements were obtained on NHPs similar to the 18
156 macaques of our study. Orange and blue dashed lines represent the step function used to describe
157 this relationship with a breakpoint at 4.5 kg. **(D)** Volumes of the tracheal (blue circles) and nasal
158 (orange triangles) regions estimated for the 18 macaques using the step function defined in the
159 subfigure C and their weights. **(E)** Mean gRNA load dynamics in nasopharyngeal (left) and
160 tracheal (right) swabs after the initial exposure to SARS-CoV-2 in naive macaques (n=6, black)
161 and after the second exposure in convalescent (n=6, blue) and $\alpha\text{CD40.RBD}$ -vaccinated
162 convalescent (n=6, green) macaques. Two additional macaques (IN + per Os, orange) were
163 initially exposed to SARS-CoV-2 via intra-nasal (0.5mL of inoculum) and intra-gastric (4.5 mL)
164 routes instead of intra-nasal (0.5 mL of inoculum) and intra-tracheal (4.5 mL) routes as defined
165 in the study. Solid lines represent mean values and error bars indicate the 5th-95th confidence
166 intervals.

167



168

169 **Fig. S10. Flow chart of the algorithm for automatic selection of covariate.**

170 At the initialization step of our study, the model without covariates is considered as initial the
 171 model, all immunological markers are seen as potential covariates (Marker) and $\{\beta, \delta\}$ is defined
 172 as the set of parameters on which covariates can be added. At each, all the marker-parameter
 173 relationships that have not already been added to the current model are added in an univariate
 174 manner to this model and ran. Among all the tested models, the one with the optimal value of
 175 selection criteria (e.g. lowest BICc) is selected (green dashed rectangle) and compared to the
 176 current model. If this one is better, it becomes the new current model and the algorithm moves to
 177 the step k+1. Otherwise, the algorithm stops.

178

179 **Table S1.** Criteria defining RBD-ACE2 binding inhibition (studies testing two-component spike nanoparticle vaccine) or
 180 neutralization measured on live cells with luciferase marker (mRNA-1273) as mechanistic correlate of protection of the effect of the
 181 vaccine on new cell infection. Studies are labelled Study 1 and Study 2 for the main and the additional studies testing two-component
 182 spike nanoparticle vaccine, respectively and mRNA-1273 for the third study evaluating several doses of mRNA-1273 vaccine.

Model		Study 1		Study 2		mRNA-1273
		RBD-ACE2 binding on β	inhibition	RBD-ACE2 binding on β	inhibition	RBD-ACE2 binding inhibition on β
Type of covariates added in the model		Time-varying	Baseline	Baseline	Baseline	Baseline
Criterion 1	Without adjustment	793.71	793.71	427.63	469.13	
	Best fits	772.34	772.34	404.80	468.70	
	(BICc Value) Adjusted for marker	765.76	765.22	413.35	467.21	
Criterion 2	Adjusted for Group	Conv: -0.747** (0.255)	Conv: -0.747** (0.255)	Vacc: -6.01**** (0.8)	10 μ g: -0.267 (0.578)	
		Conv-CD40: -2.38*** (0.265)	Conv-CD40: -2.38*** (0.265)		100 μ g: -1.6** (0.621)	
	Group effect (Value (Sd)) Adjusted for Group & marker	Conv: 0.00428 (1.71)	Conv: 0.303 (0.864)	Vacc: 2.31 (1.18)	10 μ g: 0.105(0.646)	
		Conv-CD40: 0.1 (2.79)	Conv-CD40: 0.362 (1.14)		100 μ g: 3.10-4 (0.84)	
Criterion 3	Adjusted for Group	β : 65.5 %	β : 65.5 %	β : 64.9 %	β : 18.5 %	
		δ : 54 %	δ : 54 %	δ : 58.2 %	δ : 4.6%	
	Expl. variability for β or δ (relative % ¹) Adjusted for marker	β : 87.4 %	β : 82.7 %	β : 70.8 %	β : 15.4 %	
		δ : 27.1 %	δ : 31.6%	δ : -17%	δ : 19.1 %	

¹ Relative percentage of inter-individual variability compared to variability obtained on model without any adjustment ; $100-(x*100)/ref$

* $P < 0.05$, ** $P < 0.01$, *** $P < 0.001$, **** $P < 1e-4$, Wald test for fold change different from 1

183

184

185 **Table S2.** Model parameters for viral dynamics in both the nasopharynx and the trachea
 186 estimated by the model adjusted for groups of intervention.

Param.	Meaning	Value [95% CI]	Unit
β	Infection rate in the naive group	0.95 [0.18 ; 4.94] ($\times 10^{-6}$)	(copies/ml) ⁻¹ day ⁻¹
	Fold change in the convalescent group	0.18 [0.04 ; 0.88]**	
	Fold change in the Conv-CD40 group	0.004 [0.001 ; 0.029]***	
δ	Loss rate of infected cells in the naive group	1.04 [0.79 ; 1.37]	day ⁻¹
	Fold change in the convalescent group	1.79 [1.21 ; 2.66]**	
	Fold change in the Conv-CD40 group	1.80 [1.17 ; 2.75]**	
P^N	Viral production rate in the naso.	12.1 [3.15 ; 46.5] ($\times 10^3$)	virions.(cell.day) ⁻¹
P^T	Viral production rate in the trachea	0.92 [0.39 ; 2.13] ($\times 10^3$)	virions.(cell.day) ⁻¹
$\alpha_{\text{vls g}}$	Infected cells and sgRNA viral load ratio	1.39 [1.01 ; 1.76]	Virions.cell ⁻¹
k	Eclipse rate	3	day ⁻¹
c	Clearance of <i>de novo</i> produced viruses	3	day ⁻¹
c_i	Clearance of inoculum	20	day ⁻¹
μ	Percentage of infectious viruses	10^{-3}	
$T_0^{X, nbc}$	Initial number of target cells	1.25 $\times 10^5$ (Naso.) 2.25 $\times 10^4$ (Trachea)	cells
Inoc ₀	Number of virions inoculated	2.19 $\times 10^{10}$	virions
ω_β	SD of random effect on log ₁₀ β	0.366 [0.160 ; 0.571]	
ω_δ	SD of random effect on δ	0.170 [-0.089 ; 0.429]	
σ_{VLn}	SD of error model gRNA in naso.	1.27 [1.01 ; 1.53]	
σ_{VLt}	SD of error model gRNA in trachea	1.09 [0.90 ; 1.28]	
σ_{sgVLn}	SD of error model sgRNA in naso	1.41 [0.97 ; 1.85]	
σ_{sgVLt}	SD of error model sgRNA in trachea	1.62 [1.11 ; 2.13]	

Conv-CD40 group: group of convalescent NHPs being vaccinated ; **SD:** Standard deviation ; * $P < 0.05$, ** $P < 0.01$, *** $P < 0.001$, wald test for fold change different from 1

187

188 **Table S3.** Values of -2LL estimated on models with viral clearance ($c=c_I$) and eclipse phase rate
 189 k fixed at different values.

c	k	1	3	6
1		1285.29	1286.42	1289.54
5		871.38	864.50	866.80
10		773.74	764.29	768.18
15		749.67	738.71	742.12
20		749.44	738.40	740.98
30		750.00	739.51	741.34

190

191 **Table S4.** Values of -2LL estimated on models with inoculum clearance c_I and clearance of
 192 virus de novo produced c fixed at different values. The eclipse phase rate was fixed at $k=3 \text{ day}^{-1}$.

c	c_I	1	5	10	15	20	25	30
1		1286.42	873.30	777.21	753.72	754.14	754.32	754.75
2		1286.70	864.90	760.94	734.03	734.14	733.94	734.95
3		1286.41	864.58	760.69	734.71	733.85	734.87	734.48
4		1286.33	864.22	761.78	735.91	735.16	735.42	736.14
5		1286.38	864.50	762.69	737.13	735.85	736.37	736.69
10		1286.55	865.48	764.29	738.38	737.56	737.89	738.13
15		1286.23	865.12	764.79	738.71	737.54	738.17	738.75
20		1285.96	865.19	764.78	738.86	738.40	738.25	739.30
25		1286.28	864.93	764.97	739.20	738.05	738.37	739.34
30		1286.45	864.77	765.16	739.01	738.13	738.58	739.51

193